

# Numerical Verification of Affine Systems with up to a Billion Dimensions

Stanley Bak<sup>1</sup>, Hoang-Dung Tran<sup>2</sup>, and Taylor T. Johnson<sup>2</sup>

<sup>1</sup> Safe Sky Analytics

<sup>2</sup> Vanderbilt University

**Abstract.** Affine systems reachability is the basis of many verification methods. With further computation, methods exist to reason about richer models that have inputs, nonlinear differential equations, and hybrid dynamics. As such, the scalability of affine systems verification is a prerequisite to the scalability of analysis methods for more complex systems. In this paper, we investigate these scalability limits, improving by several orders of magnitude the size of systems that can be analyzed.

One benefit of affine systems is that their reachable states can be written in terms of the matrix exponential, and safety checking can be performed at specific time steps with linear programming. Unfortunately, for large systems with many state variables, this direct approach requires an intractable amount of memory while using an intractable amount of computation time. We overcome these two problems by combining several methods that leverage common problem structure. Memory demands can be reduced by taking advantage of both initial states that are not full-dimensional, and safety properties (outputs) that only need a few linear projections of the state variables. Computation time is saved by using numerical simulations to compute only projections of the matrix exponential relevant for the verification problem. Since large systems often have sparse dynamics, we use fast Krylov-subspace simulation methods based on the Arnoldi or Lanczos iterations. Our implementation produces accurate counter-examples when properties are violated and, with sufficient problem structure, can scale to analyze systems with up to a billion real-valued state variables.

## 1 Introduction

An affine system is modeled with the ordinary differential equation  $\dot{x} = Ax + b$ , where  $x$  is a vector of  $n$  state variables,  $A$  is the  $n \times n$  dynamics matrix, and  $b$  is an  $n \times 1$  vector of constant forcing terms. Given a set of initial states, a set of unsafe states, and a time bound, the time-bounded safety verification problem is to check if there exists an initial state and a time within the bound such that the solution of the affine system enters the unsafe set.

---

DISTRIBUTION A. Approved for public release; Distribution unlimited.  
AFRL PA # 88ABW-2017-5562 cleared on 07 Nov 2017.

One way to solve the verification problem is to construct the reachable set of states. The reachable set contains all states that lie along any solutions to the differential equation  $\dot{x} = Ax + b$ , starting from any initial state up to the time bound. If the reachable set does not intersect with the unsafe states, then the system is verified as safe. In the discrete-time setting, we construct the reachable set at each time instant, and then perform the unsafe check once per step using linear programming (LP).

This discrete-time approach forms the core of many verification methods for richer classes of systems. For example, when systems have time-varying inputs, an additional input-effects term can be computed at each step and added to the discrete-time reachable set using a Minkowski sum operation [30,12]. Overapproximation of the continuous-time reachable set is possible by noting that, in the finite time between time steps, the system can only go a bounded distance from the discrete-time solution. Based on this observation, methods exist that perform bloating from the discrete-time solution in order to guarantee an overapproximation of the continuous-time reachable set [27,38,37]. The reachable set for nonlinear dynamical systems can also be overapproximated with techniques based on affine methods, by linearizing the nonlinear dynamics and then adding uncertain terms to account for mismatch between the linear and nonlinear systems. In hybridization methods [20,8,3], this process is repeated in multiple domains to reduce the overapproximation error. Finally, methods for hybrid systems that have both continuous dynamics and discrete switches [4] also build upon the core operations needed to analyze affine systems. For these systems, the reachable set is restricted to a mode’s invariant by performing set intersections, and states that reach a transition’s guard may be collected and aggregated before further computation in a successor mode. All of these powerful methods build upon the core computations used for affine systems reachability. In this paper, we focus on the scalability of this fundamental computation.

The solutions of affine systems can be written in terms of the matrix exponential, which can be used to compute the reachable set. Computation of the matrix exponential is often the main problem when systems get large. Off-the-shelf approaches to compute the matrix exponential run into two problems when applied to high-dimensional systems. First, computing the matrix exponential simply takes too much time. A simple experiment demonstrating this is shown in Figure 1, where it would take over a year to compute a single matrix exponential once a system has over ten million dimensions. Second, although the  $A$  matrix for large systems is often sparse, the matrix exponential of  $A$  will be dense. The amount of memory needed to simply store the matrix exponential result, a dense  $n \times n$  matrix, can greatly exceed what is available on modern computers, even if its computation was instant. For a million-dimensional system, this matrix would have  $10^{12}$  numbers and need about 8 TB of main memory.

To achieve scalability, we combine several existing and new methods to overcome the memory and computation time problems. The memory improvements are possible through a method that uses both aspects of reachability with support functions [38] and affine representations [36]. The computation-time im-

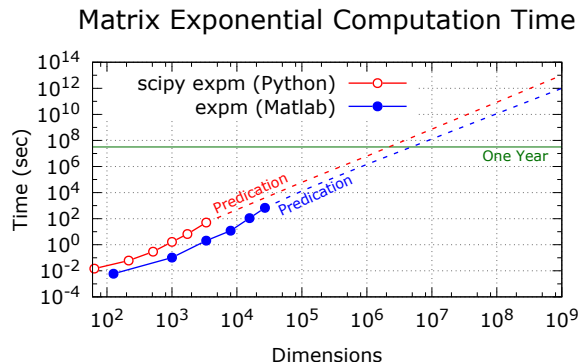


**Fig. 1.** Ignoring memory issues, off-the-shelf methods require intractable computation time to compute a single high-dimensional matrix exponential for the 3D heat diffusion system used in our evaluation.

provements use simulations to compute parts of the matrix exponential [23], possibly optimized using a new approach that simulates using the transpose system dynamics  $A^T$ . Since large dynamics matrices are often sparse (and must be sparse to simply fit into memory), we perform numerical simulations using efficient Krylov subspace methods [29,36], with modifications to reduce memory requirements for the verification problem. We propose a Cauchy error termination condition to determine when the dimension of the Krylov subspace is sufficiently large for an accurate simulation result. Individually, none of the existing methods have demonstrated scalability beyond a few thousand dimensions.

Section 2 first reviews affine discrete-time safety verification, which uses an  $n \times n$  matrix exponential at each time step. Next, Section 3 presents memory improvements followed by Section 4, which focuses on reducing computation time. The new memory scalability limits are then examined in Section 5. An evaluation on several benchmarks, some with dimension  $n$  up to one billion, is given in Section 6, followed by a review of related work and a conclusion.

## 2 Affine Verification Review

An affine, discrete-time, bounded safety verification problem is provided as input the system dynamics  $\dot{x} = Ax + b$ , a set of initial states  $\mathcal{I}$  defined as all states  $x_0$  where the linear constraints  $\mathcal{I}_x x_0 \leq \iota_x$  hold, unsafe states  $\mathcal{U}$  defined with linear constraints  $\mathcal{U}_x x \leq v_x$ , a step size  $\delta$  and time bound  $T$ . The system is called unsafe if and only if there exists a time  $t = k\delta \leq T$  such that  $x_0 \in \mathcal{I}$ ,  $x = e^{At}x_0$ , and  $x \in \mathcal{U}$ . The goal is to prove a system is safe, or find a counter-example, uniquely defined by the initial state  $x_0$  and time  $t$ .

## 2.1 Basic Verification Approach

An affine system with dynamics  $\dot{x} = Ax + b$  can be verified by first converting it to a linear system (without the  $b$  term), by adding a fresh variable to account for the effects of the forcing term  $b$ . The new  $A$  matrix has an extra column consisting of the entries of the  $b$  vector, and an extra row of all zeros. The initial value of the new variable is assigned to 1, and, since the row in  $A$  defining its differential equation is all zeros, the new variable's value remains at 1 at all times. In this way, the effect of the extra column in the  $A$  matrix is the same as the  $b$  vector in the original system. In the remainder of this paper, we consider linear systems after this transformation, assuming the form  $\dot{x} = Ax$ .

Safety can be checked by constructing a LP at each discrete time  $t$  that contains two copies of the state variables,  $x_0$  and  $x$ , and encodes the initial state conditions  $\mathcal{I}_x x_0 \leq \iota_x$ , the unsafe state conditions  $\mathcal{U}_x x \leq \upsilon_x$ , and the linear relationship (for a fixed  $t$ ) between the initial and final variables  $x = e^{At} x_0$ . If the LP is feasible, the solver provides an assignment to the variables that can be used to construct the counter-example. The bulk of the computation consists of computing  $e^{At}$  and solving an LP for each step.

In terms of efficiency improvements, note that modern LP solvers use sparse matrix representations where values of 0 in the constraints are not stored. This means that the majority of the storage cost usually comes from the matrix exponential (a dense matrix), and not the initial or unsafe state constraints. Further, since an LP solver is repeatedly invoked at many instants in time, it is more efficient to reuse the previous set of constraints and just replace the matrix exponential at each subsequent step. This also has the effect of seeding the LP solver with the closest solution from the previous time step, which greatly improves efficiency (so-called warm-start linear programming [18]). The intuition is that, for small time steps, the matrix exponential changes very little, so the point that was closest to feasible from the previous time step is often a good starting point for the next LP. Further, computing the matrix exponential often takes longer than matrix-matrix multiplication. With fixed time steps, we can compute the matrix exponential  $e^\delta$  once, and then use matrix-matrix multiplication for subsequent steps, using the fact that  $e^{A2\delta} = e^{A\delta} e^{A\delta}$ . Although this can lead to some numerical error, in practice the number of steps considered is small enough where it is usually acceptable.

## 2.2 Timed Harmonic Oscillator Example

We will use a running example of a timed harmonic oscillator to demonstrate the methods in this paper. The timed harmonic oscillator is a system with dynamics  $\dot{x} = y$ ,  $\dot{y} = -x$ , and  $\dot{t} = 1$ . For the initial set of states, take  $x_0 = -5$ ,  $y_0 \in [0, 1]$ , and  $t_0 = 0$ . The unsafe set of states consists of all states where  $x = 4$ . We attempt to verify the system with a discrete time step of  $\delta = \frac{\pi}{4}$  and a time bound of  $T = \pi$ .

On the  $x$ - $y$  plane, solutions of the system rotate clockwise around the origin. The reachable set is shown in Figure 2. From the figure, it is apparent that at time  $\frac{3\pi}{4}$ , the unsafe states are reachable.

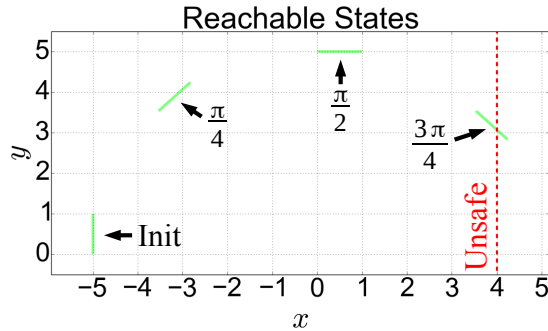


**Fig. 2.** The timed harmonic oscillator system can reach an unsafe state at time  $\frac{3\pi}{4}$ .

We can show this computationally and find the initial state that leads to the violation. First, we convert the three-variable affine system (the  $t$  variable has an affine term), to a four-variable linear system using the affine-to-linear transformation described before. The variables in the transformed system are  $\mathbf{x} = (x, y, t, a)^T$ , where  $a$  is the newly-introduced variable, which is initially 1 and remains constant at all times. The transformed dynamics now form the four-dimensional linear system  $\dot{\mathbf{x}} = A\mathbf{x}$ , with

$$A = \begin{pmatrix} 0 & 1 & 0 & 0 \\ -1 & 0 & 0 & 0 \\ 0 & 0 & 0 & 1 \\ 0 & 0 & 0 & 0 \end{pmatrix}.$$

Next, at each discrete time step, we construct the linear constraints. The constraints have two copies of the variables, one set at the initial time  $\{x_0, y_0, t_0, a_0\}$ , and one set at the current time step  $\{x, y, t, a\}$ . The linear constraints at the time of the violation,  $\frac{3\pi}{4}$ , are shown in Figure 3a. The only constraints that change between time steps are the ones encoding the matrix exponential at the current time (the values surrounded by a red rounded rectangle), for which we reuse terminology [9] and refer to as the *basis matrix*.

The linear constraints are then passed to an LP solver to check if they are feasible. For time steps 0,  $\frac{\pi}{4}$ , and  $\frac{\pi}{2}$ , the LP solver returns that no solution exists. At time  $\frac{3\pi}{4}$ , which has the constraints shown in the figure, the LP solver finds a feasible solution, and provides an assignment to the variables. In particular, its output indicates that starting from initial state  $(x_0, y_0, t_0, a_0)^T = (-5, 0.66, 0, 1)^T$ , the system can reach the unsafe state  $(x, y, t, a)^T = (4, 3.07, 2.36, 1)^T$ .

### 3 Memory Improvements

Although the basic verification approach works, it does not scale to very high dimensions. Computing and storing the basis matrix is typically the bottleneck to verification scalability. In this section we focus on the memory problem, and

$$\begin{pmatrix}
-1 & 0 & 0 & 0 & 0 \\
0 & -1 & 0 & 0 & 0 \\
0 & 0 & -1 & 0 & 0 \\
0 & 0 & 0 & -1 & 0 \\
\mathbf{1} & \mathbf{0} & \mathbf{0} & \mathbf{0} & \mathbf{0} \\
0 & \mathbf{0} & \mathbf{0} & \mathbf{0} & \mathbf{0} \\
0 & \mathbf{0} & \mathbf{0} & \mathbf{0} & \mathbf{0} \\
0 & \mathbf{0} & \mathbf{0} & \mathbf{0} & \mathbf{0} \\
0 & \mathbf{0} & \mathbf{0} & \mathbf{0} & \mathbf{0} \\
0 & \mathbf{0} & \mathbf{0} & \mathbf{0} & \mathbf{0}
\end{pmatrix}
\begin{pmatrix}
\mathbf{-0.707} & \mathbf{0.707} & \mathbf{0} & \mathbf{0} \\
\mathbf{-0.707} & \mathbf{-0.707} & \mathbf{0} & \mathbf{0} \\
\mathbf{0} & \mathbf{0} & \mathbf{1} & \mathbf{2.36} \\
\mathbf{0} & \mathbf{0} & \mathbf{0} & \mathbf{1} \\
\mathbf{0} & \mathbf{0} & \mathbf{0} & \mathbf{0} \\
\mathbf{1} & \mathbf{0} & \mathbf{0} & \mathbf{0} \\
\mathbf{0} & \mathbf{-1} & \mathbf{0} & \mathbf{0} \\
\mathbf{0} & \mathbf{1} & \mathbf{0} & \mathbf{0} \\
\mathbf{0} & \mathbf{0} & \mathbf{1} & \mathbf{0} \\
\mathbf{0} & \mathbf{0} & \mathbf{0} & \mathbf{1}
\end{pmatrix}
\begin{pmatrix}
x \\
y \\
t \\
a \\
x_0 \\
y_0 \\
t_0 \\
a_0
\end{pmatrix}
=
\begin{pmatrix}
0 \\
0 \\
0 \\
0 \\
\mathbf{4} \\
\mathbf{-5} \\
\leq \mathbf{0} \\
\leq \mathbf{1} \\
= \mathbf{0} \\
= \mathbf{1}
\end{pmatrix}$$

(a) Basic approach with full linear constraints (Section 2.1)

$$\begin{pmatrix}
-1 & \mathbf{-0.707} & \mathbf{0.707} & \mathbf{0} & \mathbf{0} \\
\mathbf{1} & \mathbf{0} & \mathbf{0} & \mathbf{0} & \mathbf{0} \\
\mathbf{0} & \mathbf{1} & \mathbf{0} & \mathbf{0} & \mathbf{0} \\
\mathbf{0} & \mathbf{0} & \mathbf{-1} & \mathbf{0} & \mathbf{0} \\
\mathbf{0} & \mathbf{0} & \mathbf{1} & \mathbf{0} & \mathbf{0} \\
\mathbf{0} & \mathbf{0} & \mathbf{0} & \mathbf{1} & \mathbf{0} \\
\mathbf{0} & \mathbf{0} & \mathbf{0} & \mathbf{0} & \mathbf{1}
\end{pmatrix}
\begin{pmatrix}
o_x \\
x_0 \\
y_0 \\
t_0 \\
a_0
\end{pmatrix}
=
\begin{pmatrix}
0 \\
\mathbf{4} \\
\mathbf{-5} \\
\leq \mathbf{0} \\
\leq \mathbf{1} \\
= \mathbf{0} \\
= \mathbf{1}
\end{pmatrix}$$

(b) Projecting onto the output space (Section 3.1)

$$\begin{pmatrix}
-1 & \mathbf{0.707} & \mathbf{3.54} \\
\mathbf{1} & \mathbf{0} & \mathbf{0} \\
\mathbf{0} & \mathbf{-1} & \mathbf{0} \\
\mathbf{0} & \mathbf{1} & \mathbf{0} \\
\mathbf{0} & \mathbf{0} & \mathbf{1}
\end{pmatrix}
\begin{pmatrix}
o_x \\
i_y \\
i_f
\end{pmatrix}
=
\begin{pmatrix}
0 \\
\mathbf{4} \\
\leq \mathbf{0} \\
\leq \mathbf{1} \\
= \mathbf{1}
\end{pmatrix}$$

(c) Projecting from the initial space onto the output space (Section 3.2)

**Fig. 3.** The linear constraints at time  $\frac{3\pi}{4}$  for the timed harmonic oscillator example described in Section 2.2 can be encoded in different ways. At each time step, only the basis matrix changes in the constraints.

show how we can reduce the height (Section 3.1) and width (Section 3.2) of the basis matrix, by taking advantage of common problem structure. In the next section we will describe how to efficiently compute the reduced size basis matrices for the verification problem.

### 3.1 Projecting onto the Output Space

First, we reduce the *height* of the basis matrix (compare the basis matrices in Figure 3a and Figure 3b). This is done by a method similar to the use of support functions with a fixed number of directions for reachability analysis [38]. The common problem structure exploited is that the verification result often only depends on a small number of directions, much smaller than the number of system variables.

Depending on the type of problem being solved (linear verification, plotting, or hybrid automaton reachability), these directions arise from different sources. For a safety verification problem for linear systems, these directions come from each of the constraints in the conjunction defining the unsafe states. For a plot, we only need to compute a projection onto the two or three plot dimensions. In this case, the important directions are the unit vectors in each of these dimensions. Plots can then be produced efficiently by running multiple optimizations

over projections of the convex reachable set at each time step [33,39]. For the hybrid automaton setting, additional directions can come from the constraints in the mode invariants, as well as from the guard conditions.

We can combine these directions into an output matrix  $C$ , where the output variables are  $y = Cx$ , and the height of the matrix is the number of output directions,  $o$ , needed for the current problem. The unsafe states,  $\mathcal{U}$ , are then redefined in the output space,  $\mathcal{U}_y y \leq v_y$ . Finally, the basis matrix in the constraints is the  $o \times n$  projection of the matrix exponential onto the output space,  $Ce^{At}$ .

Consider applying this approach to the timed harmonic oscillator system of Section 2.2, where the unsafe states are defined by  $x = 4$ . The other three dimensions,  $y$ ,  $t$ , and  $a$ , do not impact the result of the safety check, and so they (and their corresponding constraints) can be removed from the set of linear constraints, as is done in Figure 3b. In this case, the output matrix for this system is the  $1 \times 4$  matrix  $C = (1 \ 0 \ 0 \ 0)$ . We then define the unsafe states in terms of the single output space variable  $o_x$ , and replace the basis matrix by the projected matrix exponential  $Ce^{At}$ .

### 3.2 Projecting from the Initial Space

Next, we reduce the *width* of the basis matrix (compare the basis matrix in Figure 3b and Figure 3c). This is done with a method similar to reachability using affine representations [36]. The common problem structure exploited is that the initial states are often low-dimensional. For example, there may not be uncertainty in every variable, or the initial states of variables may be related.

In this case, we can define an  $i$ -dimensional initial space using an  $n \times i$  matrix  $E$ , where the initial states  $z$  are related to the original variables by  $x = Ez$ . The initial states  $\mathcal{I}$  are then redefined with constraints in the initial space,  $\mathcal{I}_z z \leq \iota_z$ . The  $o \times i$  basis matrix is computed using both projections,  $Ce^{At}E$ .

In the timed harmonic oscillator system of Section 2.2, we can define the initial states using  $i = 2$  dimensions. These are  $i_y$ , which corresponds to the initial  $y$  value, and  $i_f$  which is the fixed initial values of all the other variables. The  $E$  matrix is the  $4 \times 2$  matrix  $\begin{pmatrix} 0 & 1 & 0 & 0 \\ -5 & 0 & 0 & 1 \end{pmatrix}^T$ , and the initial constraints are  $0 \leq i_y \leq 1$  and  $i_f = 1$ . The basis matrix is the product  $Ce^{At}E$  at each step.

Using both methods, we have reduced the basis matrix from an  $n \times n$  matrix to a  $o \times i$  matrix. Importantly, we do not need both  $o$  and  $i$  to be very small for this reduction to be useful, only their *product*. Given, say, 800 MB to store the basis matrix ( $10^8$  double-precision numbers), the original approach would fill the storage when  $n = 10^4$ , a ten-thousand dimensional system. In contrast, a million-dimensional system with every dimension initially uncertain  $i = 10^6$  could still be analyzed as long as the unsafe states are defined using less than 100 independent output directions.

## 4 Computational Improvements

Although we can define the smaller basis matrix using  $Ce^{At}E$ , this does not help if we use the direct approach of computing  $e^{At}$  at each step and then multiplying

by  $C$  and  $E$ . In this section, we describe a series of improvements targeting the computational efficiency of the method.

#### 4.1 Eliminating Matrix-Matrix Multiplication

One of the efficiency improvements mentioned in Section 2.1 was to compute the matrix exponential only for the first step, and then for each subsequent step use matrix-matrix multiplication, an  $\mathcal{O}(n^3)$  operation with the usual algorithm. With low-dimensional initial and output spaces, one improvement is to do each of the subsequent steps using matrix-vector multiplications, which have a reduced per-step cost of  $\mathcal{O}(n^2)$  each. For example, if  $e^{A\delta}$  is the matrix exponential computed for the first step, after three steps the basis matrix should be  $Ce^{A\delta}e^{A\delta}e^{A\delta}E$ . By grouping operations appropriately, this computation can be done with  $3o + i$  matrix-vector multiplications:  $((Ce^{A\delta})e^{A\delta})e^{A\delta}E$ . Alternatively, if the dimensions of the initial space  $i$  is smaller than the output space  $o$ , we can group the other way and compute the basis matrix in  $3i + o$  matrix-vector multiplications:  $C(e^{A\delta}(e^{A\delta}(e^{A\delta}E)))$ . When  $n$  is large, and either  $o$  or  $i$  is small, this results in significant savings. Both of these methods, however, still require computing the full basis matrix  $e^{A\delta}$  once, which can be a space and time bottleneck when  $n$  is large.

#### 4.2 Basis Matrix using Numerical Simulations

There are many ways to compute the matrix exponential. Generally, the methods implemented in off-the-shelf libraries use a combination of squaring and scaling and Pade approximation (methods 2 and 3 [41]), which compute the entire matrix at once.

An alternative method to compute the matrix exponential uses a series of numerical simulations (method 5 [41]). The matrix exponential is computed one column at a time by using the fact that  $e^{At} = e^{At} \mathbf{I}_{n \times n} = e^{At} (\mathbf{e}_1 | \mathbf{e}_2 | \dots | \mathbf{e}_n)$ . The  $j$ th column of  $e^{At}$  is equal to  $e^{At} \mathbf{e}_j$ , where  $\mathbf{e}_j$  is the  $j$ th column of the identity matrix. The value of  $e^{At} \mathbf{e}_j$ , however, is just the solution of the linear system  $\dot{x} = Ax$  at time  $t$  from initial state  $x(0) = \mathbf{e}_j$ . To compute this, we can perform a numerical simulation with an off-the-shelf numerical method such as Runge-Kutta. This process is repeated for each column of the identity matrix to compute the full matrix exponential. For the verification problem, we need the value of  $e^{At}$  at multiple time steps, and so we run the numerical simulations up to the time bound  $T$ , recording the value at each multiple of the step size  $\delta$ . The values from each column are then combined at each multiple of time step to form the basis matrix in the LP [23].

This method can also be adapted to take advantage of the initial and output spaces. Since we need to compute the basis matrix  $Ce^{At}E$ , rather than using each column of the identity matrix, we can instead compute simulations from each column of the  $E$  matrix, and then project the state in the simulation using the  $C$  matrix. There are  $i$  columns in  $E$ , corresponding to the  $i$  dimensions of the initial states. If  $i$  is much smaller than  $n$ , this approach will be significantly faster



than computing the full matrix exponential. For the timed-harmonic oscillator system constraints in Figure 3c, for example, since the dimension of the initial space  $i = 2$ , the basis matrix could be computed in this fashion using two numerical simulations.

If the initial state dimension is large, the computation may still require a large number of simulations. This number can be reduced, however, if the output space dimension is small, by performing simulations using the transpose system dynamics. Since  $Ce^{At}E = ((Ce^{At}E)^T)^T = (E^T(e^{At})^T C^T)^T = (E^T e^{A^T t} C^T)^T$ , the basis matrix can also be computed by performing  $o$  simulations (one for each column of  $C^T$ ). These simulations use the transpose system dynamics  $A^T$ , and are projected using  $E^T$ . This allows us to compute values of the basis matrix one row at a time, and so we can compute the basis matrix using only  $o$  numerical simulations. In practice, only one of these is necessary, and so we can choose the minimum of  $i$  and  $o$  and perform that many numerical simulations, rather than computing an  $n \times n$  matrix exponential.

In the timed-harmonic oscillator system, for example, since  $o = 1$ , the entire basis matrix at each step can be computed with a single numerical simulation. The basis matrix in Figure 3c, can be computed by starting from the state from the single output direction  $(1, 0, 0, 0)^T$ , simulating using the transpose dynamics  $A^T$  up to time  $\frac{3\pi}{4}$  to get the state  $(-0.707, 0.707, 0, 0)$ , and then projecting with  $E^T = \begin{pmatrix} 0 & 1 & 0 & 0 \\ -5 & 0 & 0 & 1 \end{pmatrix}$  to get  $(0.707, 3.54)^T$ , which is the transpose of the values in the basis matrix in the constraints.

### 4.3 Simulations using the Krylov Subspace

When the system matrix  $A$  is high-dimensional, it is also often sparse (in fact, if  $A$  has more than tens of thousands of dimensions and can fit in memory, it must be sparse or otherwise compressed). We can exploit this structure to speed up numerical simulations.

The Krylov subspace simulation method [29] computes an approximation of  $e^A v$ , where  $v$  is some initial state. This is done by finding the element of the  $k$ -dimensional Krylov subspace  $K_k \equiv \text{span}\{v, Av, \dots, A^{k-1}v\}$  that best approximates  $e^A v$ .

The approximation uses a fixed number of iterations of the well-known Arnoldi algorithm [7]. The Arnoldi algorithm computes an orthonormal basis for the Krylov subspace  $K_k$  by starting with a normalized version of  $v$  as both the first orthonormal direction and the current vector and, at each iteration, (1) multiplying the current vector by  $A$ , (2) projecting out the previous orthonormal directions from the current vector, (3) normalizing the current vector, and (4) adding it to the list of orthonormal directions. After  $k$  iterations, the two outputs are  $V_k$ , the  $n \times k$  matrix of orthonormal basis vectors, and  $H_k$  the  $k \times k$  matrix that is a projection of the linear transformation  $A$  in the Krylov subspace  $K_k$ .

The outputs of the Arnoldi algorithm can be used to approximate  $e^A v$ . This is done by projecting the initial state into the (smaller) Krylov subspace, computing the matrix exponential using the projected linear transformation  $H_k$ , and then projecting the result back to the higher-dimensional space using  $V_k$ . By the

design of the Krylov subspace, the projection of the initial state  $v$  is just the length of  $v$  multiplied by the first unit vector in the subspace,  $\mathbf{e}_1$ . Further, since for any time  $t$ , the Krylov subspaces associated with  $A$  and  $At$  are identical, we can use the same  $V_k$  and  $H_k$  to compute the approximation at any point in time. Note, however, that different initial states have different Krylov subspaces, so a new  $V_k$  and  $H_k$  must be computed for each simulation. The full formula for the approximation is given by:

$$e^{At}v \approx \|v\| V_k e^{H_k t} \mathbf{e}_1 \quad (1)$$

The above approximation formula is especially useful when the size of  $A$  is huge, e.g., millions of dimensions, since it transforms the computation with a huge matrix  $A$  to a problem with a much smaller matrix  $H_k$ . For fast computation, we would like to minimize the size of  $H_k$  by using a small number of Arnoldi iterations  $k$ , but this has the effect of reducing the approximation accuracy [28]. Thus, it is critical to select  $k$  large enough to be accurate, but small enough to be fast. An a priori error bound of the approximation [29] is given by

$$2 \|v\| \frac{\|At\|^k e^{\|At\|}}{k!}. \quad (2)$$

We could think to use this bound to determine the number of iterations when the error of the approximation would be below some small value. Alternatively, we could fix the number of iterations, and then bloat the reachable set by the priori error bound to ensure the true solution is contained in the computed reachable set overapproximation. Such approaches for reachability have been considered [36], but unfortunately the a priori error bound can be very pessimistic. For example, consider a 40x40x40 version of the 3D heat diffusion system used in our evaluation. At time 500, this system has matrix norm  $\|At\| = 100704.5$ . For an initial unit vector with  $\|v\| = 1$ , even after a large number of Arnoldi iterations  $k = 20000$ , the computed error bound from Equation 2 is effectively unusable,  $10^{66459}$ . One can try to overcome this by using a better a priori error bound if the matrix meets additional structure requirements [2].

Alternatively, instead of using an a priori error bound, we propose an a posteriori approach based on the Cauchy error in the resultant simulation. This is similar to how Krylov methods are used in iterative methods for solving sparse problems in linear algebra, where the number of iterations is increased until the change in the answer becomes acceptably small.

We use the Krylov simulation method to compute a column of the basis matrix at each time step using both  $k - 1$  and  $k$  Arnoldi iterations. If the difference between the results at all time steps is small, we stop. Otherwise, we increase  $k$  and try again.

One problem that can arise is that, when  $k$  is very small, the output of the simulation is the zero vector. This can be because either that particular initial dimension has no effect on the outputs, or because  $k$  was too small. To resolve this, we can insert an additional output direction with a vector of all ones, so that a change will likely be detected in the output as long as any state variable

### Heat 50x50x50 Simulation Accuracy

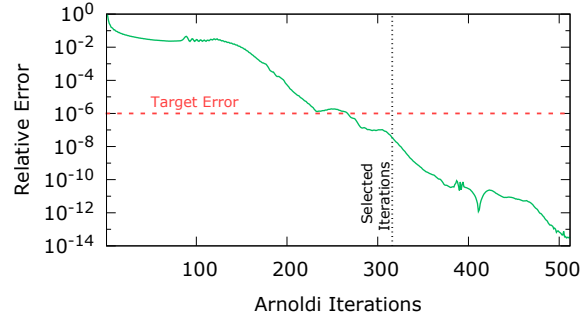


**Fig. 4.** The simulation error tuning approach stops at 316 Arnoldi iterations for the 125000-dimensional system.

changes. Alternatively, if we know that all initial directions will affect some output, we can simply increase  $k$  when the simulation output is the zero vector.

The convergence of the Krylov simulation error in the limit can be guaranteed theoretically by noting that the a priori error bound from Equation 2 still applies, and it converges to zero in the limit. More strongly, once the number of Arnoldi iterations reaches the number of system variables  $n$ , the Krylov subspace process is just a change of basis, and the error will be zero. In practice, the error threshold is reached much faster than either of these two conditions.

For the 3D heat diffusion system we will use in our evaluation, the relative error between  $k$  and  $k + 1$  with the vector of ones added as an output direction is shown in Figure 4. In the implementation, we start with  $k = 4$  and increase it by factors of 1.5 until the desired relative error threshold,  $10^{-6}$  (the tolerance used in our LP solver), is achieved, but going no larger than  $n$ . In the figure, the method stopped upon reaching 316 iterations, which has error below the threshold.

When using the Krylov simulation approach, we must still perform many (smaller) matrix exponential operations to compute  $e^{H_k t}$  at each time step. However, since we are actually computing  $e^{H_k t} \mathbf{e}_1$  for each time step  $t$ , we can reuse the enhancements previously described in Section 4.1 and Section 4.2. In particular, we can compute the matrix exponential once, and then do repeated matrix-vector multiplication to get the value at each of the subsequent steps. Alternatively, we can use a numerical simulation of a smaller system where  $H_k$  is the system dynamics matrix and  $\mathbf{e}_1$  is the initial state.

A further enhancement is possible when the system matrix is both sparse and symmetric. This may be the case when the system matrix comes from a physical system due to the symmetry of many physical laws. In this case, the Arnoldi iteration can be replaced by the more efficient Lanczos iteration. The difference between the two is that  $H$  matrix in the symmetric case is tridiagonal. This means that that step (2) in the algorithm, projecting out the previous

orthonormal directions from the current vector, only needs to be done for the previous two directions, and only requires a single further dot product. This reduces the computation time from  $\mathcal{O}(k^2)$  to  $\mathcal{O}(k)$ , and presents an opportunity to save significant memory. Since we eventually project the result of  $V_k e^{H_k t} \mathbf{e}_1$  onto the output space matrix  $C$  (or the transpose of the initial space matrix  $E^T$ ), we can embed this projection into the Lanczos iteration at each step. This eliminates the need to store  $V_k$ , a potentially large  $n \times k$  matrix, and the modified Lanczos iteration will then output  $H_k$  and the projected  $CV_k$  (or  $E^T V_k$ ).

## 5 Memory Scalability Limits

Several variables have been defined that impact the scalability of the proposed approach:  $n$ , the number of dimensions in the system dynamics,  $i$ , the initial space dimensions,  $o$ , the output space dimensions,  $s$ , the number of discrete time steps, and  $k$ , the dimension of the Krylov subspace used in the simulations, which is equal to the number of Arnoldi or Lanczos iterations needed. Except for  $k$ , these are static variables, known before any computation is performed. Using these variables, we can define the memory needed for the computation.

The amount of memory needed to store the basis matrix for all the steps is:

$$o \times i \times s \times \text{sizeof}(\text{double}) \quad (3)$$

Importantly, this limit is independent of the system dimensions  $n$ , which is why analysis with the proposed approach can scale to extremely large systems. In this case, even if one of  $o = n$  or  $i = n$ , analysis may still be possible, as long as the product of  $i$  and  $o$  is manageable.

Next, if performing the Arnoldi iteration, we must also store  $H_k$ , a  $k \times k$  matrix, and  $V_k$ , an  $n \times k$  matrix. The memory used by the Arnoldi algorithm is:

$$k \times (n + k) \times \text{sizeof}(\text{double}) \quad (4)$$

The  $k \times n$  factor in this equation is often the bottleneck, meaning that successful high-dimensional system analysis cannot require a too high-dimensional Krylov subspace.

In the modified Lanczos iteration,  $H_k$  is tridiagonal, and instead only the projection of  $V_k$  is stored. During the iteration, the current and previous two vectors of  $V$  must be stored in order to be projected out, so a further factor of  $3n$  is also needed. The memory required for the Lanczos iteration is:

$$(3k + (n \times o) + 3n) \times \text{sizeof}(\text{double}) \quad (5)$$

If the transpose system simulation is used,  $o$  is replaced by  $i$ .

Finally, the system matrix  $A$  and initial space and output matrices  $E$  and  $C$  also need to fit into memory. Even with a sparse representation, this can take non-negligible memory when systems are very large.

## 6 Evaluation

We evaluate the proposed approach using several high-dimensional benchmarks. Measurements were performed on a system with a 12-core Intel i7-5930K processor with a large 128 GB of main memory.

### 6.1 Modified Nodal Analysis (MNA5)

We first verify a benchmark model based on a system from the field of electrical circuit analysis, where the state variables relate to the node voltage and currents inside a circuit [15,45]. Originally a DAE system, the dynamics matrix has been adapted to create a benchmark for verification using ODE reachability methods. In this system,  $n = 10923$ ,  $o = 2$ ,  $i = 10$ ,  $s = 20000$ . As far as we are aware, this benchmark is the largest linear system ever verified [9], where the safe version previously took a little over 24 hours. Our implementation automatically selected  $k = 63$  using the Krylov simulation error tuning approach, and verified the safe version of this system in 3.2 *seconds*. The unsafe version of the benchmark was checked in 0.9 seconds, generating a counter-example at the same time in the analysis as the earlier approach, at exactly step 1919. The relative error between the computed counter-example and an external numerical simulation was  $1.2 \times 10^{-9}$ , demonstrating the accuracy of the proposed approach.

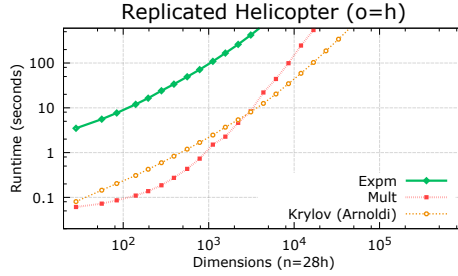
### 6.2 Replicated Helicopter

A tunable benchmark is created based on a 28-dimensional helicopter model and controller<sup>3</sup>. The helicopter is copied multiple times within the same model, in order to create a verification problem that can scale to an arbitrary number of dimensions. SpaceEx [27] and Hylaa [10] were previously evaluated on this system, and in about 10 minutes of runtime, successfully verified versions with several hundreds of dimensions [11].

In the replicated helicopter benchmark, the 28-dimensional helicopter model is copied  $h$  times, so that the number of dimensions  $n = 28h$ . For each helicopter  $j$ , we add a single term to the error condition conjunction  $x_8^j \geq 0.45$ , so that the output dimension  $o = h$ . We take the initial conditions from the `x8_over_time_large` configuration, where eight of the variables for each helicopter are initially intervals, making the dimension of initial space  $i = 8h$ . Finally, the problem calls to verify up to time 30 with a step of 0.1, so that the number of steps  $s = 300$ .

Note this is a particularly bad case for our analysis method, since both  $i$  and  $o$  increase as we add more helicopters. We can compute a bound on the maximum number of helicopters using Equation 3. Our 128 GB of main memory would be exhausted for storing the basis matrices when the number of helicopters  $h = 2675$ , a system with about 75 thousand dimensions.

<sup>3</sup> <http://spaceex.imag.fr/news/helicopter-example-posted-39>



Dims	Expn	Mult	Kry
28	3.49	<b>0.06</b>	0.08
140	12.0	<b>0.11</b>	0.31
1120	109	<b>1.51</b>	2.47
3108	421	8.44	<b>8.09</b>
12040	-	245	<b>58.8</b>
33068	-	-	<b>340</b>

**Fig. 5.** With one output for each helicopter,  $o = h$ , the `Krylov` method can verify the replicated helicopter system with around 40000 dimensions in 10 minutes.

**Table 1.** Replicated Helicopter Runtime (sec) with  $o = h$

In 10 minutes of runtime, we could verify a system with about 40 thousand dimensions, as shown in Figure 5. In the plot, `Expn` performs a full matrix exponential at each step for computing the basis matrix (Section 2.1), `Mult` performs a single matrix exponential at the first step and then uses  $o$  matrix-vector multiplications for each remaining step (Section 4.1), and `Krylov` uses the Arnoldi simulation method (Section 4.3).

We also analyzed a modified version of the benchmark, where the unsafe condition is changed to check the average of the  $x_8^j$  variables, making the output dimension  $o = 1$ . This improves scalability by both reducing the size of the basis matrix, and, since we can do simulations in the transpose dynamics, by reducing the number of required simulations to 1. The memory bottleneck is lifted, and the new computational bottleneck becomes the LP solving step. We can successfully analyze this system with around 300 thousand dimensions in 10 minutes. Further details for this version of the system are presented in Appendix A.1.

### 6.3 3D Heat Diffusion

We next consider a three-dimensional heat diffusion benchmark taken from the field of partial differential equations (PDEs). This benchmark is based on a two-dimensional version that has previously been analyzed up to a  $50 \times 50$  mesh (2500 dimensions) [34,36]. The problem is to examine the temperature at the center point of a  $1.0 \times 1.0 \times 1.0$  block, where one of a portion of the block is initially heated. As before, all of the sides of the block are insulated except the  $x = 1.0$  edge, which allows for heat exchange with the ambient environment with a heat exchange constant of 0.5. A heated initial region is present in the region where  $x \in [0.0, 0.4]$ ,  $y \in [0.0, 0.2]$ , and  $z \in [0.0, 0.1]$ . The heated region temperature is between 0.9 and 1.1, with the rest of material initially at temperature 0.0. The system dynamics is given by the PDE  $u_t = \alpha^2(u_{xx} + u_{yy} + u_{zz})$ , where  $\alpha = 0.01$  is the diffusivity of the material, as in the previous work.

A linear state space model of the system is obtained using the semi-finite difference method [26], discretizing the block with a  $m \times m \times m$  grid. This

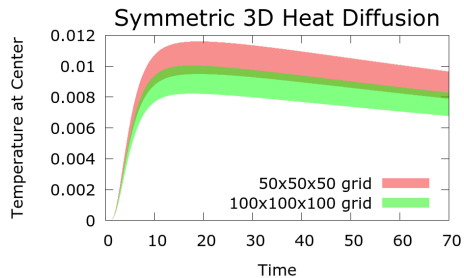


**Fig. 6.** The maximum temperature at the center point occurs around time 15.

$m$	Temp	$k$	Lanczos	Arnoldi
10	0.02966	63	0.5s	0.3s
20	0.01716	94	0.5s	0.4s
50	0.01161	211	1.3s	6.7s
100	0.01005	474	7.4s	6m28s
200	0.00933	711	1m40s	2h3m
500	0.00891	1599	45m55s	-
1000	0.00877	3597	13h26m	-

**Table 2.** Symmetric 3D Heat Diffusion with  $n = m^3$  Dimensions

results in an  $m^3$ -dimensional linear state space model describing the evolution of the temperature at each mesh point.

Due to the initially heated region, we expect the temperature at the center of the block to first increase, and then decrease due to the heat loss along the  $x = 1$  edge. Further, there may be error due to the space discretization step, so if  $m$  is too small, the model does not accurately predict the behavior of the PDE. We can see both of these effects by computing and plotting the reachable states, as shown in Figure 6. Since the peak temperature happens at around time  $t = 15$ , we perform further analysis by running the system with max time  $T = 25.0$  and step  $\delta = 0.025$ , making the number of steps  $s = 1000$ . This system presents a particularly good case for our analysis method, since  $i = 1$ ,  $o = 1$ , and the dynamics matrix is symmetric which allows us to use the more efficient Lanczos iteration. The runtimes and temperatures reachable for various values of  $m$  are given in Table 2. Accurate analysis requires high dimensions, motivating the need for the types of analysis methods developed in this paper.

The  $1000 \times 1000 \times 1000$  version can be analyzed using our approach in a little over 13 hours of computation time. In this case, each of the billion rows of the  $A$  matrix generally has 7 entries, so that simply storing the elements of the matrix (8 bytes per double-precision number) consumes 56 GB of RAM (this could be reduced by about half by using data structures that take advantage of the symmetry). Further, since a 3597-dimensional Krylov subspace is needed, the Arnoldi iteration would be infeasible for this system, as it would require storing 3597 vectors for the  $V$  matrix, each of which contains a billion numbers (8 GB each), for a total memory requirement of 28 TB (recall Equation 4).

We also analyzed a non-symmetric version of this system, where the heated region is replaced by a permanent heater along on the bottom of the block, along the 2D rectangle where  $x \in [0.0, 0.4]$  and  $y \in [0.0, 0.2]$ . In this case, the Krylov Arnoldi method succeeded in analyzing the 100x100x100 system (one million dimensions) in about 5 minutes. Further details are available in Appendix A.2.

## 7 Related Work

The proposed method uses convergent numerical schemes to compute simulations as part of a verification procedure. Convergent numerical schemes have been used before to approximate reachable sets of nonlinear hybrid systems, in particular, level-set methods that approximate solutions to Hamilton-Jacobi PDEs [40,44,13]. Other methods for this class of systems also use simulations for formal analysis, where individual executions are bloated according to model-specific discrepancy functions [24], as implemented in tools such as C2E2 [22,25]. Another analysis approach for nonlinear systems uses Taylor models, such as those in Flow\* [16], which can scale to around ten real variables ( $\mathbb{R}^{10}$ ) [17]. Specializing to affine dynamics, as recently as 2011 the state-of-the-art for reachability computation was on the order of a hundred real variables ( $\mathbb{R}^{100}$ ) [27].

Our work uses the Krylov subspace to simulate high-dimensional systems, which is often also used in model order reduction methods [6]. Notice that in our case, since each simulation has a different Krylov subspace, there is no single reduced order model that can be constructed and analyzed. Model-order reduction approaches verify a smaller dimensional model [19], and can sometimes use an error bound to compute a guaranteed overapproximation of the original full-order system [35,34,46]. Such approximation methods may be formalized as sound abstractions or developed in the context of approximate simulation and bisimulation relations [31,32]. Model order reduction methods have verified linear systems with on the order of a thousand real variables ( $\mathbb{R}^{1000}$ ).

Our approach to verification is similar to the Hylaa tool [10], which has verified systems with up to ten thousand dimensions ( $\mathbb{R}^{10000}$ ) [9,12]. Another recent work decomposes systems using a series of two-dimensional projections, and has also scaled to analyze systems of this magnitude with modest increases in overapproximation error [14]. We scale to larger systems than these approaches by leveraging initial and output spaces and Krylov simulations.

We use numerical simulations to compute  $e^{At}v$ . This operation is sometimes called the action of a matrix on vector  $v$ , and methods exist for its efficient computation [1,43]. Profiling against Python’s matrix action implementation (`scipy.sparse.linalg.expm_multiply`) indicated that, for high-dimensional systems, Krylov methods were faster.

Due to the reliance on simulations with error estimates, we call the proposed method *numerical verification*, which contrasts with more traditional verification methods that achieve conservative error bounds through bloating. The cost of these conservative methods, though, is that they do not produce counterexamples when systems are classified as unsafe. The estimate of computation accuracy in our approach is tunable, for example, up to the accuracy of the LP solver, or up to floating-point precision. Given that the dynamics matrix is provided in floating point, and in practice modeling errors can be much larger, we believe this remains useful. For large systems, the only analysis option we are aware of beyond simple simulation would be a falsification method [5,21,42], which runs individual simulations trying to optimize towards an unsafe region. Unlike our approach, these methods do not exhaustively explore the state space.



In the context of existing work, our contribution is, under the right conditions, the analysis of affine systems with up to a billion real variables ( $\mathbb{R}^{1000000000}$ ), a seven-fold order of magnitude improvement beyond the state-of-the-art from just a half decade ago ( $\mathbb{R}^{100}$ ), and a five-fold order of magnitude improvement from the past year ( $\mathbb{R}^{10000}$ ).

## 8 Conclusion

The state-space explosion problem usually prevents analysis of high-dimensional systems. In order to achieve scalability, we exploited up to four types of problem structure: (i) a small dimension of initial states, (ii) a small dimension of the output space, (iii) the sparsity of the system  $A$  matrix, and (iv), optionally, the symmetry of the  $A$  matrix. When problems have this structure, it is possible to efficiently perform verification or plot projections of reachable states in very high dimensions. As the structure assumptions are violated, the proposed approach degrades gracefully, requiring more computation time and memory depending on the degree of the violation. We have shown the method's effectiveness by analyzing systems with up to a billion continuous dimensions.

## References

1. A. H. Al-Mohy and N. J. Higham. Computing the action of the matrix exponential, with an application to exponential integrators. *SIAM journal on scientific computing*, 33(2):488–511, 2011.
2. M. Althoff. Reachability analysis of large linear systems with uncertain inputs in the krylov subspace. *arXiv preprint arXiv:1712.00369*, 2017.
3. M. Althoff, O. Stursberg, and M. Buss. Reachability analysis of nonlinear systems with uncertain parameters using conservative linearization. In *Decision and Control, 2008. CDC 2008. 47th IEEE Conference on*, pages 4042–4048. IEEE, 2008.
4. R. Alur, C. Courcoubetis, T. A. Henzinger, and P.-H. Ho. Hybrid automata: An algorithmic approach to the specification and verification of hybrid systems. In *Hybrid systems*, pages 209–229. Springer, 1993.
5. Y. Annpureddy, C. Liu, G. Fainekos, and S. Sankaranarayanan. S-taliro: A tool for temporal logic falsification for hybrid systems. In *International Conference on Tools and Algorithms for the Construction and Analysis of Systems*, pages 254–257. Springer, 2011.
6. A. C. Antoulas, D. C. Sorensen, and S. Gugercin. A survey of model reduction methods for large-scale systems. *Contemporary Mathematics*, 280:193–219, 2001.
7. W. E. Arnoldi. The principle of minimized iterations in the solution of the matrix eigenvalue problem. *Quarterly of applied mathematics*, 9(1):17–29, 1951.
8. S. Bak, S. Bogomolov, T. A. Henzinger, T. T. Johnson, and P. Prakash. Scalable static hybridization methods for analysis of nonlinear systems. In *International Conference on Hybrid Systems: Computation and Control*, 2016.
9. S. Bak and P. S. Duggirala. Direct verification of linear systems with over 10000 dimensions. In *4th International Workshop on Applied Verification of Continuous and Hybrid Systems*, EPiC Series in Computing. EasyChair, 2017.

10. S. Bak and P. S. Duggirala. Hylaa: A tool for computing simulation-equivalent reachability for linear systems. In *Proceedings of the 20th International Conference on Hybrid Systems: Computation and Control*. ACM, 2017.
11. S. Bak and P. S. Duggirala. Rigorous simulation-based analysis of linear hybrid systems. In *International Conference on Tools and Algorithms for the Construction and Analysis of Systems*. Springer, 2017.
12. S. Bak and P. S. Duggirala. Simulation-equivalent reachability of large linear systems with inputs. In *Proceedings of the 29th International Conference on Computer Aided Verification*. Springer, 2017.
13. S. Bansal, M. Chen, S. Herbert, and C. J. Tomlin. Hamilton-Jacobi reachability: A brief overview and recent advances. *arXiv preprint arXiv:1709.07523*, 2017.
14. S. Bogomolov, M. Forets, G. Frehse, A. Podelski, C. Schilling, and F. Viry. Reach set approximation through decomposition with low-dimensional sets and high-dimensional matrices. In *Proceedings of the 21st International Conference on Hybrid Systems: Computation and Control*. ACM, 2018.
15. Y. Chahlaoui and P. Van Dooren. A collection of benchmark examples for model reduction of linear time invariant dynamical systems. 2002.
16. X. Chen, E. Abraham, and S. Sankaranarayanan. Taylor model flowpipe construction for non-linear hybrid systems. *Real-Time Systems Symposium*, 2012.
17. X. Chen, S. Schupp, I. B. Makhlof, E. Ábrahám, G. Frehse, and S. Kowalewski. A benchmark suite for hybrid systems reachability analysis. In *NASA Formal Methods Symposium*, pages 408–414. Springer, 2015.
18. J. W. Chinneck. Practical optimization: a gentle introduction. *Systems and Computer Engineering*.
19. Y. Chou, X. Chen, and S. Sankaranarayanan. A study of model-order reduction techniques for verification. In *International Workshop on Numerical Software Verification*, pages 98–113. Springer, 2017.
20. T. Dang, O. Maler, and R. Testylier. Accurate hybridization of nonlinear systems. In *International conference on Hybrid systems: computation and control*, 2010.
21. A. Donzé. Breach, a toolbox for verification and parameter synthesis of hybrid systems. In *International Conference on Computer Aided Verification*, pages 167–170. Springer, 2010.
22. P. S. Duggirala, S. Mitra, M. Viswanathan, and M. Potok. C2E2: a verification tool for stateflow models. In *International Conference on Tools and Algorithms for the Construction and Analysis of Systems*, pages 68–82. Springer, 2015.
23. P. S. Duggirala and M. Viswanathan. Parsimonious, simulation based verification of linear systems. In *International Conference on Computer Aided Verification*, pages 477–494. Springer, 2016.
24. C. Fan and S. Mitra. Bounded verification with on-the-fly discrepancy computation. In *International Symposium on Automated Technology for Verification and Analysis*, pages 446–463. Springer, 2015.
25. C. Fan, B. Qi, S. Mitra, M. Viswanathan, and P. S. Duggirala. Automatic reachability analysis for nonlinear hybrid models with C2E2. In *International Conference on Computer Aided Verification*, pages 531–538. Springer, 2016.
26. S. J. Farlow. *Partial differential equations for scientists and engineers*. Courier Corporation, 1993.
27. G. Frehse, C. Le Guernic, A. Donzé, S. Cotton, R. Ray, O. Lebeltel, R. Ripado, A. Girard, T. Dang, and O. Maler. Spaceex: Scalable verification of hybrid systems. In *International Conference on Computer Aided Verification*. Springer, 2011.
28. E. Gallopoulos and Y. Saad. On the parallel solution of parabolic equations. In *Proceedings of the 3rd international conference on Supercomputing*. ACM, 1989.

29. E. Gallopoulos and Y. Saad. Efficient solution of parabolic equations by krylov approximation methods. *SIAM Journal on Scientific and Statistical Computing*, 13(5):1236–1264, 1992.
30. A. Girard, C. Le Guernic, and O. Maler. Efficient computation of reachable sets of linear time-invariant systems with inputs. In *International Workshop on Hybrid Systems: Computation and Control*, pages 257–271. Springer, 2006.
31. A. Girard and G. J. Pappas. Approximation metrics for discrete and continuous systems. *Automatic Control, IEEE Transactions on*, 52(5):782–798, 2007.
32. A. Girard and G. J. Pappas. Approximate bisimulation: A bridge between computer science and control theory. *European Journal of Control*, 17(5):568–578, 2011.
33. A. Gurung and R. Ray. An efficient algorithm for vertex enumeration of two-dimensional projection of polytopes. *CoRR*, abs/1611.10059, 2016.
34. Z. Han. *Formal verification of hybrid systems using model order reduction and decomposition*. PhD thesis, Dept. of ECE, Carnegie Mellon University, 2005.
35. Z. Han and B. Krogh. Reachability analysis of hybrid control systems using reduced-order models. In *American Control Conference, 2004. Proceedings of the 2004*, volume 2, pages 1183–1189. IEEE, 2004.
36. Z. Han and B. H. Krogh. Reachability analysis of large-scale affine systems using low-dimensional polytopes. In *HSCC*, volume 6, pages 287–301. Springer, 2006.
37. C. Le Guernic. *Reachability analysis of hybrid systems with linear continuous dynamics*. PhD thesis, Université Joseph-Fourier-Grenoble I, 2009.
38. C. Le Guernic and A. Girard. Reachability analysis of linear systems using support functions. *Nonlinear Analysis: Hybrid Systems*, 4(2):250–262, 2010.
39. A. V. Lotov, V. A. Bushenkov, and G. K. Kamenev. *Interactive decision maps: Approximation and visualization of Pareto frontier*, volume 89. Springer Science & Business Media, 2013.
40. I. Mitchell and C. Tomlin. Level set methods for computation in hybrid systems. In *HSCC*, volume 1790, pages 310–323. Springer, 2000.
41. C. Moler and C. Van Loan. Nineteen dubious ways to compute the exponential of a matrix, twenty-five years later. *SIAM review*, 45(1):3–49, 2003.
42. A. Rizk, G. Batt, F. Fages, and S. Soliman. On a continuous degree of satisfaction of temporal logic formulae with applications to systems biology. In *International Conference on Computational Methods in Systems Biology*, pages 251–268. Springer, 2008.
43. R. B. Sidje. Expokit: a software package for computing matrix exponentials. *ACM Transactions on Mathematical Software (TOMS)*, 24(1):130–156, 1998.
44. C. Tomlin, I. Mitchell, A. Bayen, and M. Oishi. Computational techniques for the verification of hybrid systems. *Proceedings of the IEEE*, 2003.
45. H.-D. Tran, L. V. Nguyen, and T. T. Johnson. Large-scale linear systems from order-reduction (benchmark proposal). In *3rd Applied Verification for Continuous and Hybrid Systems Workshop (ARCH), Vienna, Austria*, 2016.
46. H.-D. Tran, L. V. Nguyen, W. Xiang, and T. T. Johnson. Order-reduction abstractions for safety verification of high-dimensional linear systems. *Discrete Event Dynamic Systems, Special Issues on Formal Method in Control, to appear*, 2017.

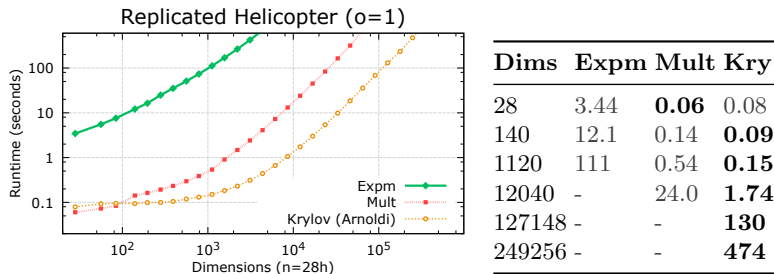


**Fig. 7.** With smaller output space  $o = 1$ , the Krylov method verify the replicated helicopter system with about 300 thousand dimensions in 10 minutes (top of the y axis).

**Table 3.** Replicated Helicopter Runtime (sec) with  $o = 1$

## A Additional Experiments

### A.1 Replicated Helicopter with Combined Error Condition

We considered a modified version of the helicopter benchmark, where the unsafe condition is changed to check the average of the  $x_s^j$  variables, making the output dimension  $o = 1$ . From Equation 3, we now would exhaust main memory storing the basis matrices when  $h \approx 7.15$  million, a system with about 200 million dimensions.

Analysis of the runtime for this version of the benchmark is shown in Figure 7. In the larger systems, solving the LP becomes the bottleneck, making improvements to the Arnoldi portion less important.

### A.2 Nonsymmetric 3D Heat Diffusion

We analyzed a non-symmetric version of the 3D Heat Diffusion system, where the initially heated region is replaced by a permanent heater is present along on the bottom of the block  $z = 0.0$ , along the 2D rectangle where  $x \in [0.0, 0.4]$  and  $y \in [0.0, 0.2]$ . We analyze the system up to time 500, with a time step of 0.5 ( $s = 1000$ ). The plot of the temperature reachable at the center for the  $10 \times 10 \times 10$  version (1000 dimensions) and the  $100 \times 100 \times 100$  version (1 million dimensions) is shown in Figure 8. Table 4 shows the maximum temperature reached at the center of the block as we vary the number of mesh points per axis  $m$ .

The scalability bottleneck for this system comes from the memory needed for the Arnoldi algorithm as given in Equation 4. The  $200 \times 200 \times 200$  version exhausted memory before completing.

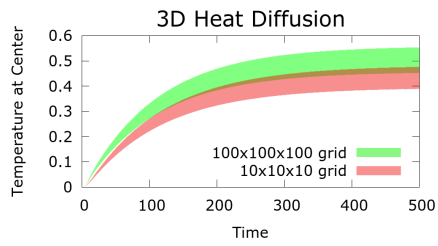


**Fig. 8.** The spatial discretization affects the temperature reachable at the center.

$m$	Temp	$k$	Runtime
5	0.4389	28	0.2s
10	0.4762	63	0.2s
20	0.5142	141	0.7s
50	0.5423	316	13.7s
100	0.5534	474	5m41s

**Table 4.** 3D Heat Diffusion with  $n = m^3$  Dimensions